

Phase Adjustment of S-Parameters from Coupled Resonator Filters

L. M. da Silva¹ , M. T. de Melo¹ , M. G. A. R. Santos² , A. J. R. Serres² 

¹Department of Electronics and Systems, Federal University of Pernambuco, Recife, Brazil,
leomoraasilva@gmail.com, marcostdemelo@gmail.com

²Electrical engineering department, Federal University of Campina Grande, Campina Grande, Brazil,
gmarilialves@gmail.com, alexandreserres@dee.ufcg.edu.br

Abstract— This paper presents a method to cancel the constant phase loading and transmission line that are added to the S-parameters of coupled resonant networks. Thus, the phase-corrected S-parameters may be used to obtain a rational model together with its representative coupling matrix. This method is applicable to lossy and lossless coupled resonator networks with two ports, such as microwave filters. In addition, it has the advantage of not requiring S-parameters with wide frequency ranges, and offers less computational effort than other approaches. Examples including simulations of microwaves passband filters are provided in order to demonstrate the effectiveness of this new technique.

Index Terms— Coupling matrix, filters, rational approximation, vector fitting.

I. INTRODUCTION

It is well known that the S-parameters of a linear, discrete and time-invariant network may be modeled by rational functions in the frequency domain. In addition, for coupled resonant filters, these rational models may be analytically related to a coupling matrix (CM) [1]. As this matrix has a direct application in the computer-aided tuning (CAT) of resonant filters [2], this relationship has been exploited by several authors to extract the coupling matrix from the frequency response of a filter. However, the S-parameters obtained from coupled resonant filters differ from their ideal model due to two non-ideal effects [3]: 1) a constant phase loading that is created by higher order modes present near input/output (I/O) coupling elements, and 2) a section of embedded transmission line at each filter port. Since both effects cause an additional phase shift in the filter S-parameters, it must be eliminated in order to obtain a correct rational model of the device [3]. Therefore, some methodologies have been proposed in order to solve the problem. An estimated value for the additional phase shift was presented in [3] employing a curve adjustment of the group delay of S_{11} at frequency points at a distance from the central frequency of the filter. In references [4]-[6], the additional phase shift is obtained by minimizing an objective function defined as the difference between the initial S-parameters and those obtained from the extracted coupling matrix model. In reference [7], the additional phase shift is indirectly eliminated by exhaustively solving a least-square problem. Lastly, reference [8] uses vector fitting (VF) [9] to obtain a high-order rational network model, and select the poles and zeros located far from the origin in order to generate the values of the additional phase shift. The inversion of the extracted coupling matrix embedded in the operations

presented in [4]-[6] may be considered as a problem. This inversion impairs the convergence of the algorithm, particularly for high-order filters, since the number of operations needed to mount the objective function increases as the filter order increases. In relation to [3], [7] and [8], the authors claim that the input S-parameters require a frequency range that varies from 3 to 6 times the filter bandwidth. This may therefore represent a limitation in cases where the available input S-parameters are defined in shorter frequency ranges.

To overcome these problems, we propose a new method based on the minimization of an error function, where there are no embedded matrix inversion operations. Compared to [4]-[6], this method reduces operational costs and is less susceptible to convergence problems. Moreover, and unlike the methods in [3], [7] and [8], the proposed method does not demand wide frequency ranges for the input S-parameters.

II. THEORY

A model for a two-port coupled filter of order N is presented in Fig. 1[1]. The circuit comprises a series of N individual first-degree lowpass sections connected in parallel between the source and load terminations. Each section comprises one parallel-connected capacitor C_k and one susceptance b_k [1], connected through admittance inverters of characteristic admittances M_{Sk} and M_{Lk} . In addition, a direct source-load coupling inverter M_{SL} [1] is included to allow fully canonical transfer functions to be realized.

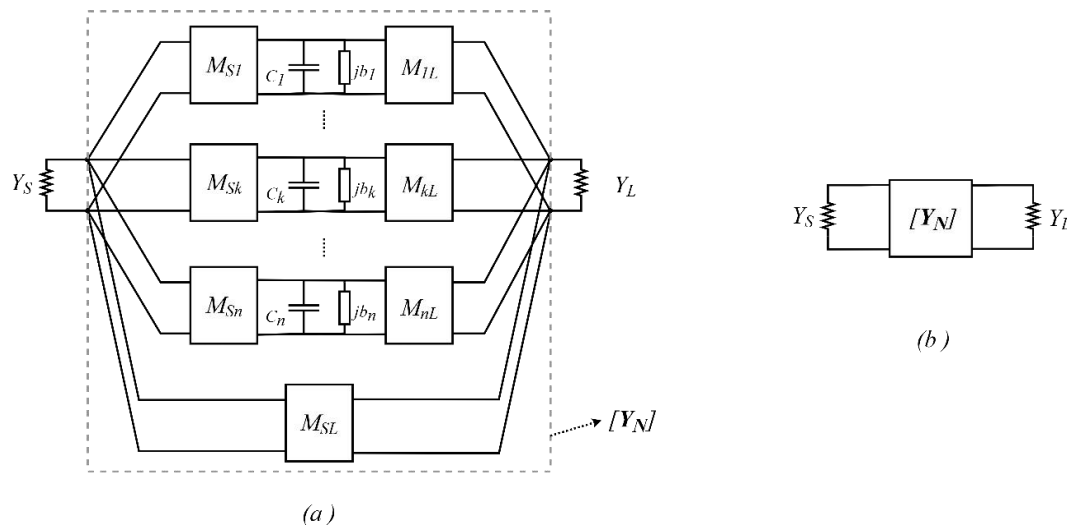


Fig. 1. Equivalent circuit of an N coupled-resonator network. (a) Detailed representation. (b) Black box representation.

Expression (1) is the two-port short-circuited admittance matrix $[Y_N]$ of the circuit presented in Fig. 1[1]. It is the sum of the Y-parameter matrices for the N individual sections, plus the Y-parameter matrix $[y_{SL}]$ for the admittance inverter of characteristic admittance M_{SL} . Still in relation to (1), M_{kk} is the self-coupling of resonator “k”, and Ω is the low pass normalized frequency variable.

$$[Y_N] = j \begin{bmatrix} 0 & M_{SL} \\ M_{SL} & 0 \end{bmatrix} + \sum_{k=1}^N \frac{1}{\Omega + jM_{kk}} \begin{bmatrix} M_{Sk}^2 & M_{Sk}M_{kL} \\ M_{Sk}M_{kL} & M_{kL}^2 \end{bmatrix} \quad (1)$$

Expression (1) establishes a relationship between the residues r_{11k} , r_{21k} and r_{22k} of the two-port matrix $[Y_N]$. This relation is given by (2),

$$r_{11k} = \frac{r_{21k}^2}{r_{22k}} \quad (2)$$

where r_{11k} , r_{21k} and r_{22k} appear in the pole-residue expansion of the matrix $[Y_N]$, given by (3) [1]. As an observation, it is evident that $M_{SL}=K$ and $M_{kk}=jp_k$. Still in relation to (3), p_k is the k -th pole of the expansion and K is a factor that must be included in the expansion in order to model fully canonical transfer functions [1].

$$[Y_N] = \frac{1}{y_d} \begin{bmatrix} y_{11n} & y_{21n} \\ y_{12n} & y_{22n} \end{bmatrix} = \begin{bmatrix} 0 & K \\ K & 0 \end{bmatrix} + \sum_{k=1}^N \frac{1}{\Omega - p_k} \begin{bmatrix} r_{11k} & r_{21k} \\ r_{12k} & r_{22k} \end{bmatrix} \quad (3)$$

Figure 2 presents the equivalent circuit when the existence of phase shift in the filter S-parameters is considered. For this case, the two-port Y matrix may be converted to the ABCD matrix and use the cascade multiplication proprieties of ABCD matrix to show that the two-port short-circuited admittance matrix $[Y_N']$ no longer has the form of (1). The consequence of this is that (2) must not be true. We propose therefore to use this feature to estimate the additional phase shift in the filter S-parameters.

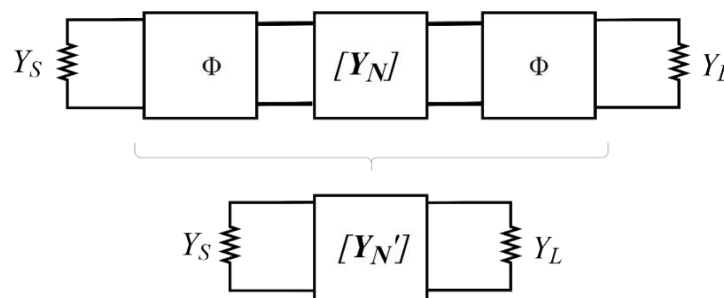


Fig. 2. Equivalent circuit of a network with embedded phase delay.

A. Defining the error function

The proposed method is outlined in Fig.3.

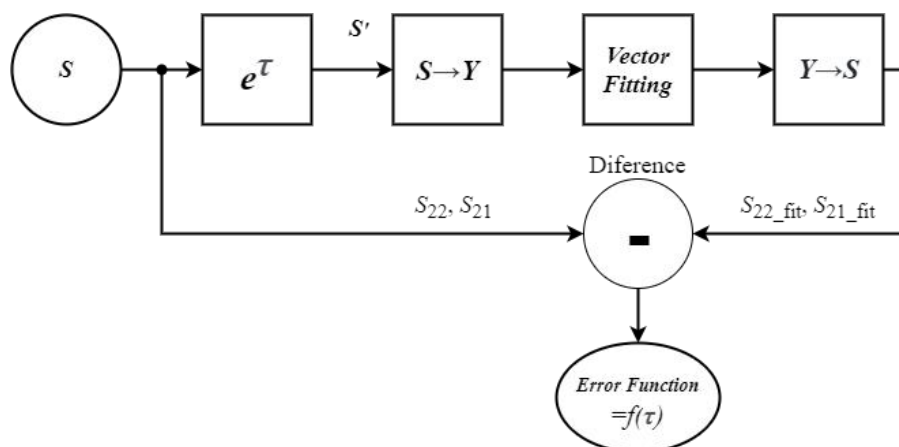


Fig. 3. Block diagram of the proposed method.

According to Fig. 3, the error function (or error) is defined as the difference between the initial S-

parameters and those generated from a rational model obtained by vector fitting (VF) [10] by considering a given additional phase shift in the S-parameters. Thus, the error depends on parameter τ , which represents the additional phase shift. For networks with two ports, τ is a two element vector given by $[\tau_1 \ \tau_2]$, such that $\tau_i = j(\varphi_i + \theta_i f / f_c)$ where φ_i and θ_i are constants to be determined and f_c and f are, respectively, the central operating frequency of the filter and the passband frequency variable. It may be noted that φ_i and θ_i represent a constant phase loading and a section of a transmission line that are proposedly added in the filter S-parameters in order to cancel the non-ideal effects. This is outlined in Fig. 4.

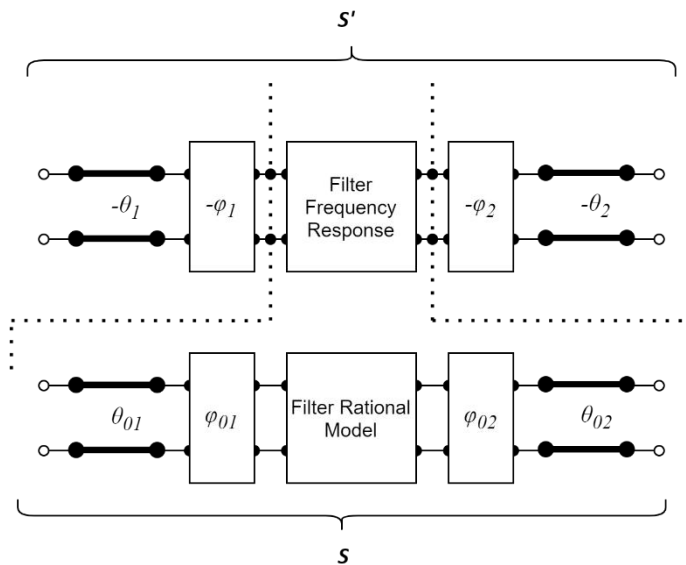


Fig. 4. Block diagram of the filter with phase delay removal.

From Fig. 4, the phase corrected S-parameters (S') may be given by (4).

$$[S'] = \begin{bmatrix} e^{-\tau_1} & 0 \\ 0 & e^{-\tau_2} \end{bmatrix} [S] \begin{bmatrix} e^{-\tau_1} & 0 \\ 0 & e^{-\tau_2} \end{bmatrix} \quad (4)$$

After this step, S' is converted into Y-parameters, using the classic two-port S matrix for Y matrix transformation formulas [11] with normalized characteristic impedances. Thus, using VF, the rational model presented in (5) must be extracted for Y_{21} and Y_{22} , where N is the filter order.

$$[Y] = \frac{1}{y_d} \begin{bmatrix} y_{21n} \\ y_{22n} \end{bmatrix} = \begin{bmatrix} K \\ 0 \end{bmatrix} + \sum_{k=1}^N \frac{1}{\Omega - p_k} \begin{bmatrix} r_{21k} \\ r_{22k} \end{bmatrix} \quad (5)$$

With r_{21k} , r_{22k} , it is possible to obtain the residues of the expansion of parameters Y_{11} (i.e., r_{11k}) from (2). Consequently, the extracted model for Y_{11} is obtained using (6). The extracted model for Y_{21} , Y_{22} and Y_{11} is used to obtain the extracted scattering parameters S_{22_fit} and S_{21_fit} and define the error function $f(\tau)$ from (7), where N_p is the number of simulated (or measured) points.

$$Y_{11}(\Omega) = \sum_{k=1}^N \frac{r_{11k}}{\Omega - p_k} \quad (6)$$

$$f(\tau) = \sum_{i=1}^{N_p} \left(\left| |S_{22}(\Omega_i)| - |S_{22_fit}(\Omega_i)| \right| + \left| |S_{21}(\Omega_i)| - |S_{21_fit}(\Omega_i)| \right| \right) \quad (7)$$

Still in relation to (7), $|x|$ is the absolute value of a scalar “x”, and Ω_i is the i -th point for the normalized frequency variable so that $S_{ij}(\Omega_i)$ represents the value of the scattering parameter S_{ij} at Ω_i . When the values chosen for τ do not cancel the effects caused by the transmission line section or the phase loading on the filter ports (i.e., $\theta_i \neq \theta_{0i}$, or $\varphi_i \neq \varphi_{0i}$ in Fig. 4), the parameters Y_{11} obtained using (6) will be incorrect. This makes S_{22_fit} and S_{21_fit} different from S_{22} and S_{21} and demonstrates that the non-removal of φ_{0i} and θ_{0i} from the S-parameters leads to incorrect rational models for Y_{11} . Hence, the main idea behind this method is to find the values of φ_i and θ_i (with $i = 1, 2$) in order to minimize (7). When this minimization is performed, (6) is validated and a correct S-parameters model for the filter is obtained. As a consequence, the values of the poles and residues of Y_{21} and Y_{22} may be used to obtain the transverse coupling matrix of the network (see [1]).

B. Minimizing the error function

In order to minimize the error function, and consequently find the values of φ_i and θ_i , an optimization tool may be used. The data set to be used for the optimization, i.e., the frequency range of the input S-parameters, may be defined as that range of sampled Y-parameters that encompasses all the peaks in the Y_{22} and Y_{21} responses, without being unnecessarily large. For example, good results were obtained using the range presented in Fig. 5 where the lower interval frequency, f_{min} , is such that the inclination of $\text{abs}(Y_{22}(f_{min}))$ or $\text{abs}(Y_{21}(f_{min}))$ is equal to 10° , and the upper interval frequency, f_{max} , is such that the inclination of $\text{abs}(Y_{22}(f_{max}))$ or $\text{abs}(Y_{21}(f_{max}))$ is equal to 170° .

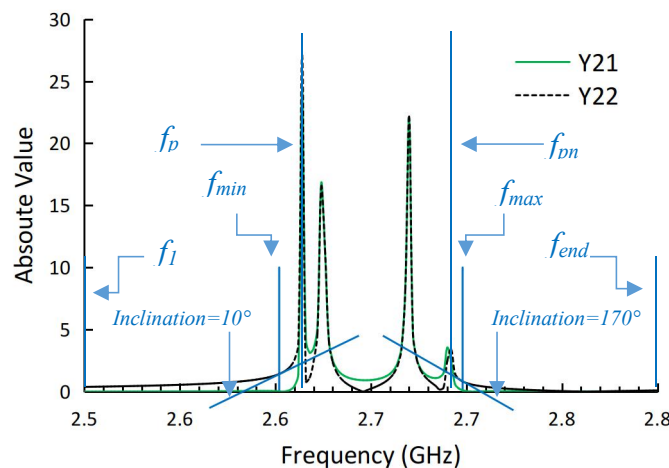


Fig. 5 Generic Y_{21} and Y_{22} responses.

In Fig. 5, it is possible to observe that $f_{min} \in [f_1 \ f_{p1}]$ and $f_{max} \in [f_{pn} \ f_{end}]$, where f_1 and f_{end} , are, respectively, the minimum and maximum frequency points of the input data set, and f_{p1} and f_{pn} are, respectively, the first and last frequency point at which $\text{abs}(Y_{22})$ or $\text{abs}(Y_{21})$ are peaks. Using this criterion, it is possible to ensure a small enough frequency range, which encompasses all the poles of

the Y-parameters for the rationalization process. To ensure convergence of the optimization process, we used (8) with δ equal to a low value, such as 0.005 (error of 0.5%).

$$f(\gamma) \leq \text{error} = 2\delta \times N_p \quad (8)$$

In this work, the Nelder-Mead simplex algorithm [12] was chosen as the optimization tool, since it is easy to understand and implement.

III. EXAMPLES

In this section, three examples are presented to demonstrate the effectiveness of the proposed method. For each case, it was possible to obtain the correct rational model, and make a comparison between its frequency responses with the original filters' response. The following steps were used in order to perform this task:

- 1) Create an error function $f(\tau)$ given by (7). This function must be in function of $\varphi_1, \theta_1, \varphi_2, \theta_2$;
- 2) Estimate the frequency range of the input S-parameters (f_{\min} and f_{\max}), using Sec II, item B;
- 3) Numerically minimize error function $f(\tau)$ using the Nelder-Mead simplex algorithm with the sampled data obtained in step 2 and stop when (8) has become satisfied.

A. Fourth-order lossless cross-shaped filter

The fourth-order cross-shaped filter was designed to have $f_c = 2.535$ GHz, $\text{FBW} = 2.7617\%$, $N_z = 2$ (two finite transmission zeros), and RL_{\max} (maximum return loss in passband) given by 20 dB. The microstrip board had: $\epsilon_r = 2.94$, $d = 1.524$ mm, $\tan(\delta) = 0$, and $\sigma = \infty$ (metallization with infinite conductivity). This way the filter geometry is shown in Fig. 6, where $a = 4.8$ mm, $b = 3.8$ mm, $c = 2.2$ mm, $w = 1.0$ mm, $w_{LT} = 1.5$ mm, $L_{LT} = 11.9$ mm, $g_1 = g_4 = 0.2$ mm, $g_2 = g_3 = 0.3$ mm, $d_{12} = d_{34} = 1.7$ mm, $d_{23} = 1.5$ mm, and $d_{14} = 2.2$ mm.

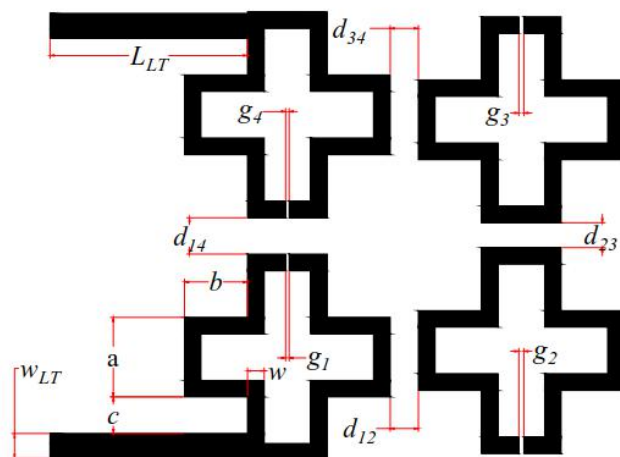


Fig. 6. Fourth order filter layout.

The filter S-parameters were obtained for 201 frequency points by using a full-wave EM simulation tool in the range of 2.4 GHz to 2.8 GHz. Thus, the proposed method was applied for two situations: a) considering the frequency range calculated using the criterion shown in Fig. 5; and b) using the total frequency range available. In case a), it was possible to find $\varphi_i = 131.5534^\circ$ and $\theta_i = -106.4002^\circ$ so

that $f(\gamma) = 0.139 < \text{error} = 0.49$ with $f_{\min} = 2.498$ GHz, $f_{\max} = 2.594$ GHz and $N_p = 49$. In case b), it was possible to find $\varphi_i = 125.3633^\circ$ and $\theta_i = -100.2402^\circ$ so that $f(\gamma) = 1.3744 < \text{error} = 2.01$ with $f_{\min} = 2.4$ GHz, $f_{\max} = 2.8$ GHz and $N_p = 201$. With this, Figs. 7, 8 and 9 present comparisons between the rational model and the original (simulated) parameters.

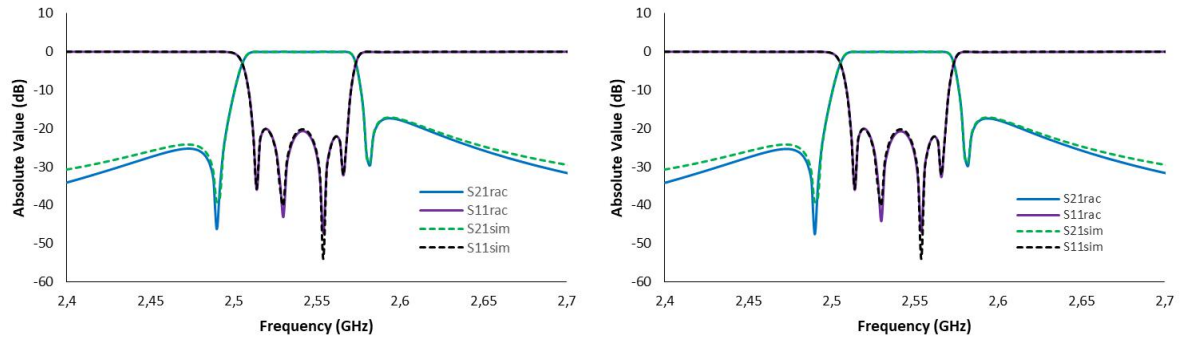


Fig. 7. Absolute value of the fourth order filter S-parameters (lossless case). The left for $f_{\min} = 2.498$ GHz, $f_{\max} = 2.594$ GHz. The right, for $f_{\min} = 2.4$ GHz, $f_{\max} = 2.8$ GHz.

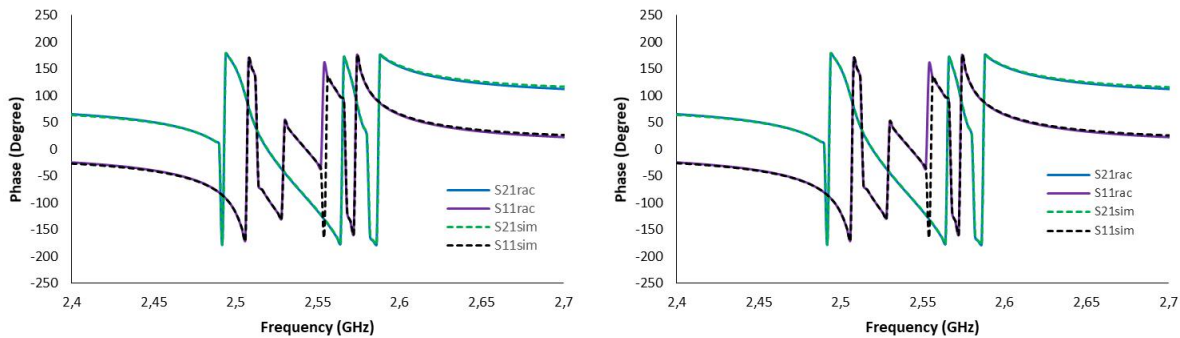


Fig. 8. Phase of the fourth order filter S-parameters (lossless case). The left for $f_{\min} = 2.498$ GHz, $f_{\max} = 2.594$ GHz. The right, for $f_{\min} = 2.4$ GHz, $f_{\max} = 2.8$ GHz.

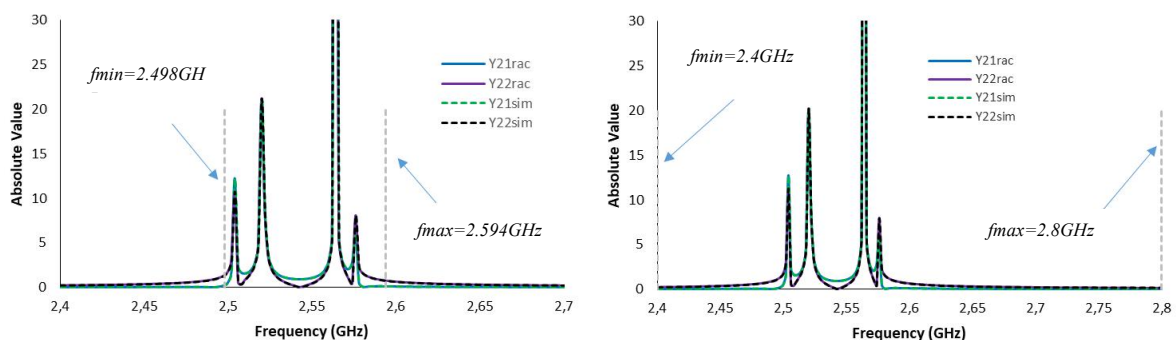


Fig. 9. Absolute value of the fourth order filter Y-parameters (lossless case). The left for $f_{\min} = 2.498$ GHz, $f_{\max} = 2.594$ GHz. The right, for $f_{\min} = 2.4$ GHz, $f_{\max} = 2.8$ GHz.

In Figs. 7, 8 and 9, a very good agreement may be observed between the rationalized and the original responses, hence, the reduced frequency range ($f_{\min} = 2.498$ GHz, $f_{\max} = 2.594$ GHz) is sufficient to generate an accurate rational model. However, it may also be observed that there is some mismatch between these curves at the rejection bands, even when the total frequency range available

is used. The origin of this difference is due to two limitations: a) The model proposed in [1] for coupled resonator filters (Fig. 1) loses precision at frequencies that are far from the central filter frequency; b) The model proposed in [3] for the nonlinearities existing in the filter S-parameters is empirical, and therefore, not exact. As a result, both effects create a systematic error that does not decrease even when the data range (f_{\min} to f_{\max}) is increased. Fortunately, the combined effect of these limitations is small and does not present a problem for the proposed application.

The folded $N+2$ coupling matrix is obtained from the extracted rational model by using the formulation in [13]. Thus, the coupling matrix as well as its external quality factors [14] were extracted, and are summarized in Table I.

TABLE I. COUPLING MATRIX AND EXTERNAL QUALITY FACTORS

M_{ij}	$j=1$	$j=2$	$j=3$	$j=4$
$i=1$	-0.0042 (exr)	0.0187(exr)	0.0000(exr)	-0.0072(exr)
	-0.0041 (ext)	0.0187(ext)	0.0000(ext)	-0.0072(ext)
	0.0000 (id)	0.0192(id)	0.0000(id)	-0.0068 (id)
	0.0187(exr)	-0.0018(exr)	0.0181(exr)	0.0035(exr)
$i=2$	0.0187(ext)	-0.0017(ext)	0.0181(ext)	0.0035(ext)
	0.0192(id)	0.0000(id)	0.0188(id)	0.0000 (id)
	0.0000(exr)	0.0181(exr)	-0.0089(exr)	0.0184(exr)
$i=3$	0.0000(ext)	0.0181(ext)	-0.0089(ext)	0.0184(ext)
	0.0000 (id)	0.0188(id)	0.0000(id)	0.0192 (id)
	-0.0072(exr)	0.0035(exr)	0.0184(exr)	-0.0041(exr)
$i=4$	-0.0072(ext)	0.0035(ext)	0.0184(ext)	-0.0040(ext)
	-0.0068 (id)	0.0000 (id)	0.0192 (id)	0.0000 (id)
Q_1	41.9920(exr)			42.0191(exr)
	41.0130(ext)		Q_2	41.9964(ext)
	41.9170(id)			41.9170(id)

In Table I, suffix *exr* indicates extracted parameters using the reduced frequency range, suffix *ext* indicates extracted parameters using the total frequency range available, and suffix *id* signifies ideal parameters. As expected, by analyzing Figs. 7, 8 and 9, the extracted coupling matrix and the extracted quality factors do not differ significantly for the three situations. One further observation regarding the extracted coupling matrix is the evident existence of different types of coupling, since Hong [14] demonstrated that electrical and magnetic couplings have opposite signs for open loop coupled resonators.

B. Fourth-order lossy cross-shaped filter

In this example, the same model presented in Example A is used, however, considering the presence of dielectric and metallization losses (respectively expressed by $\tan(\delta) = 0.0012$ for the dielectric and $\sigma=5,80e7$ S/m for the metallization). By using the proposed method, the following was found: a) $\varphi_i = 136.8578^\circ$ and $\theta_i = -111.9402^\circ$ so that $f(\gamma) = 0.1653 < \text{error} = 0.52$ for $f_{\min} = 2.492$ GHz, $f_{\max} = 2.594$ GHz and $N_p = 52$; and $\varphi_i = -66.2687^\circ$, and b) $\theta_i = -88.5748^\circ$ so that $f(\gamma) = 1.6761 < \text{error} = 2.01$ for $f_{\min} = 2.4$ GHz, $f_{\max} = 2.8$ GHz and $N_p = 201$. For both cases, in Figs. 10, 11 and 12, a good

agreement is evident between the extracted rational model and the original filter response.

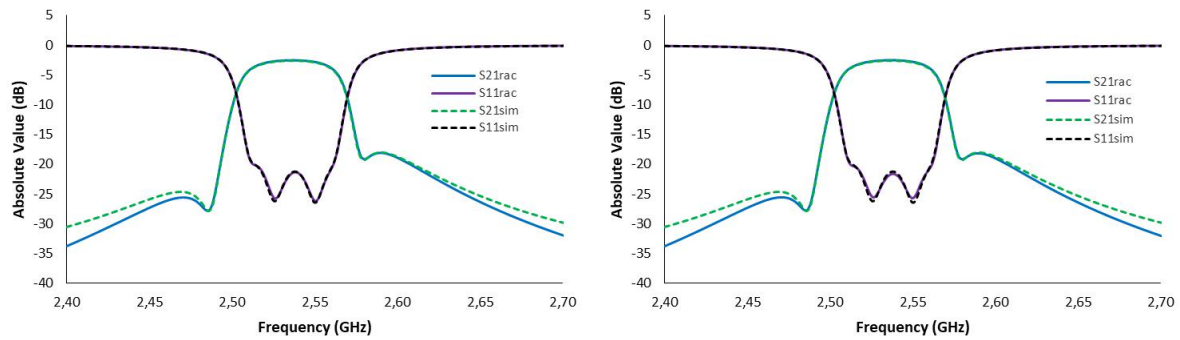


Fig. 10. Absolute value of the fourth order filter S-parameters (lossy case). The left for $f_{\min} = 2.492$ GHz, $f_{\max} = 2.594$ GHz. The right, for $f_{\min} = 2.4$ GHz, $f_{\max} = 2.8$ GHz.

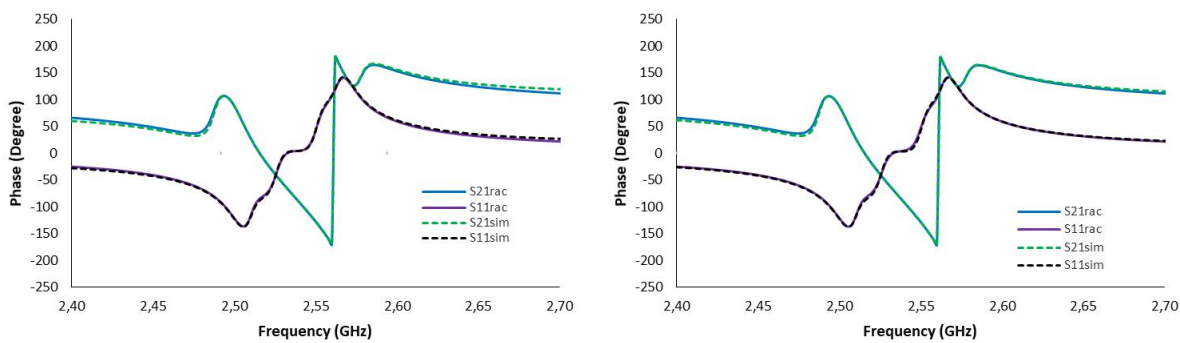


Fig. 11. Phase of the fourth order filter S-parameters (lossy case). The left for $f_{\min} = 2.492$ GHz, $f_{\max} = 2.594$ GHz. The right, for $f_{\min} = 2.4$ GHz, $f_{\max} = 2.8$ GHz.

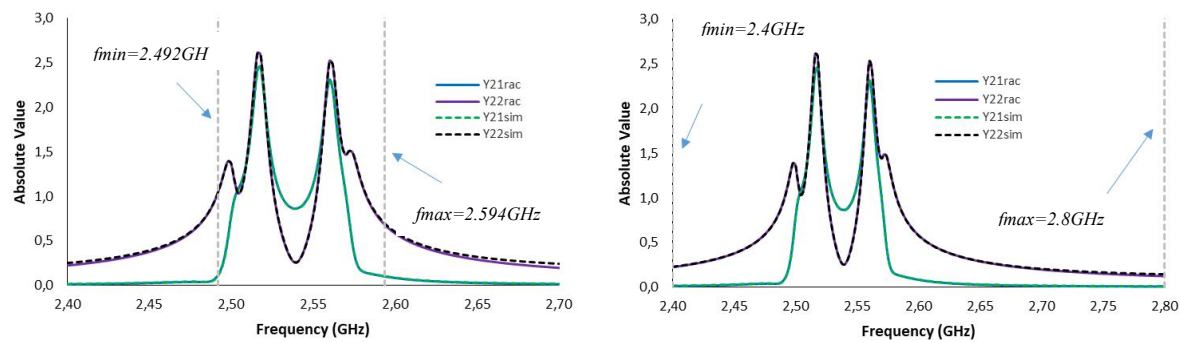


Fig. 12. Absolute value of the fourth order filter Y-parameters (lossless case). The left for $f_{\min} = 2.492$ GHz, $f_{\max} = 2.594$ GHz. The right, for $f_{\min} = 2.4$ GHz, $f_{\max} = 2.8$ GHz.

The coupling matrix as well as the external quality factors for this are given in Table II, where complex elements are now added to the main diagonal. As previously shown in [10], these elements are related to the losses. One further observation is that there is no significant change in the value of the real part of M_{ij} when compared to Example A. This indicates that the losses have little influence on the self and mutual couplings between the resonators.

TABLE II. EXTRACTED COUPLING MATRIX AND EXTERNAL QUALITY FACTORS

Mij	j=1	j=2	j=3	j=4
i=1	-0.0014-j0.0038(exr)	0.0187(exr)	0.0000(exr)	-0.0072(exr)
	-0.0013-j0.0037(ext)	0.0186(ext)	0.0000(ext)	-0.0072(ext)
i=2	0.0187(exr)	-0.0010-j0.0037(exr)	0.0181(exr)	0.0035(exr)
	0.0186(ext)	-0.0010-j0.0037(ext)	0.0180(ext)	0.0035(ext)
i=3	0.0000(exr)	0.0181(exr)	-0.0062-j0.0036(exr)	0.0184(exr)
	0.0000(ext)	0.0180(ext)	-0.0061-j0.0035(ext)	0.0184(ext)
i=4	-0.0072(exr)	0.0035(exr)	0.0184(exr)	-0.0014-j0.0037(exr)
	-0.0072(ext)	0.0035(ext)	0.0184(ext)	-0.0012-j0.0039(ext)
Q ₁	42.2120(exr)		Q ₂	41.8725(exl)
	42.3960(ext)			41.8232(ext)

C. Sixth order lossy cross-shaped filter.

In this example, the proposed method is used when the S-parameters are from a sixth order lossy filter. The filter has six poles, four transmission zeros and was designed to have $f_c = 1.50$ GHz, FBW = 3.00% and $RL_{max} = 20$ dB. This is presented in Fig.13, where $c = 1.6$ mm, $w_{LT} = 0.7$ mm, $L_{LT} = 14.7$ mm, $g_1 = g_6 = 0.9$ mm, $g_2 = g_5 = 1.0$ mm, $g_3 = g_4 = 1.1$ mm, $d_{12} = d_{56} = 0.5$ mm, $d_{23} = d_{45} = 0.8$ mm, $d_{34} = 0.4$ mm, $d_{16} = d_{25} = 2.0$ mm, and each cross resonator has the same dimensions of Example A.

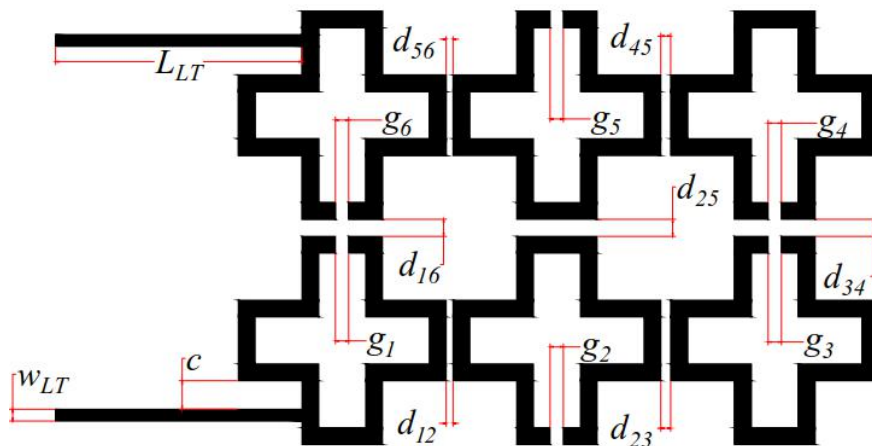


Fig. 13. Sixth order filter layout.

For this filter, the simulation was performed for 201 frequency points in the range 1.4 GHz to 1.6 GHz with a microstrip board of $\epsilon_r = 9.2$, $d = 0.762$ mm, $\tan(\delta) = 0.0001$ and with copper metallization with $\sigma = 5.80 \times 10^7$ S/m. Thus, using the proposed method, it was possible to find: a) $\varphi_i = 128.5626^\circ$ and $\theta_i = -103.9855^\circ$ so that $f(\gamma) = 0.1009 < \text{error} = 0.6$ for $f_{min} = 1.468$ GHz, $f_{max} = 1.527$ GHz and $N_p = 60$; and b) $\varphi_i = -71.8242^\circ$ and $\theta_i = -71.8242^\circ$ so that $f(\gamma) = 1.4383 < \text{error} = 2.01$ for $f_{min} = 1.4$ GHz, $f_{max} = 1.6$ GHz and $N_p = 201$. With this, Figs. 14, 15 and 16 present comparisons between the rational model and the original (simulated) parameters.

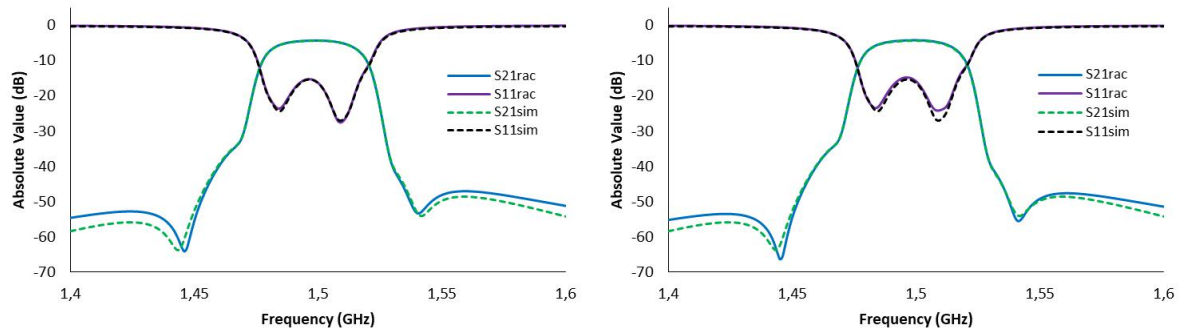


Fig. 14. Absolute value of the sixth order filter S-parameters. The left for $f_{\min} = 1.468$ GHz, $f_{\max} = 1.527$ GHz. The right, for $f_{\min} = 1.4$ GHz, $f_{\max} = 1.6$ GHz.

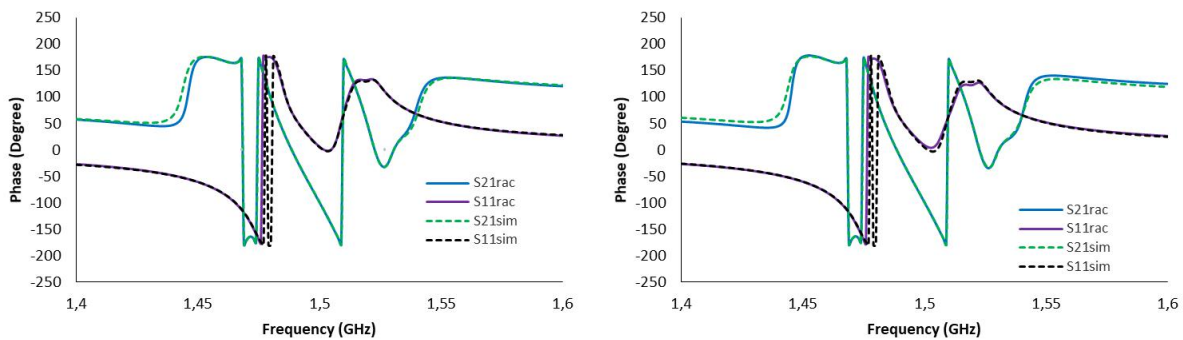


Fig. 15. Phase of the sixth order filter S-parameters (lossy case). The left for $f_{\min} = 1.468$ GHz, $f_{\max} = 1.527$ GHz. The right, for $f_{\min} = 1.4$ GHz, $f_{\max} = 1.6$ GHz.

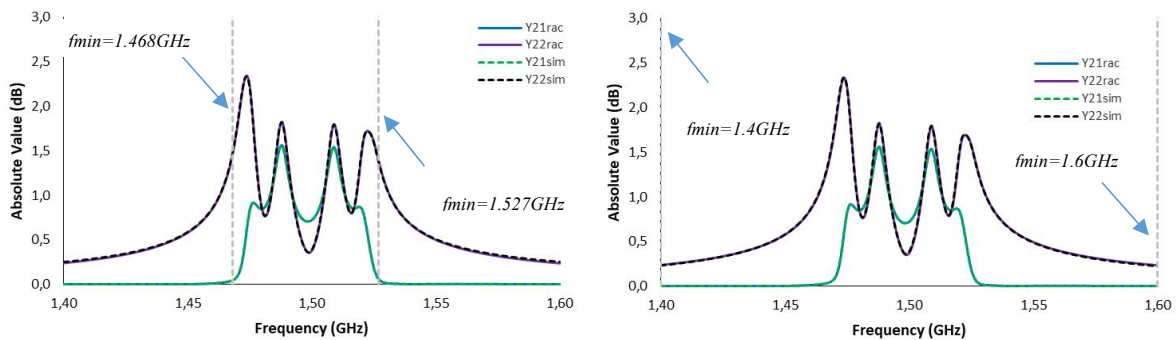


Fig. 16. Absolute value of the sixth order filter Y-parameters. The left for $f_{\min} = 1.468$ GHz, $f_{\max} = 1.527$ GHz. The right, for $f_{\min} = 1.4$ GHz, $f_{\max} = 1.6$ GHz.

As occurred in Examples A and B, in the present case, a good agreement may be observed between the rational and simulated responses, indicating that the extracted rational model is correct. In addition, it may also be observed that the reduced frequency range ($f_{\min} = 1.468$ GHz, $f_{\max} = 1.527$ GHz) is sufficient to generate an accurate rational model.

The coupling matrix as well as the external quality factors for this case are given in Table III. The suffixes *extr*, *ext* and *id* are described in example A, and all M_{ij} must be multiplied by 10^{-3} . From Table III, it may be observed that the coupling matrix and external quality factors are close to their ideal values. In addition, the coupling matrix is almost symmetric in relation to the secondary diagonal. This fact contributes to the veracity of the model, since the structure in Fig. 13 is symmetrical with respect to the feed lines.

TABLE III. EXTRACTED COUPLING MATRIX AND EXTERNAL QUALITY FACTORS

M_{ij}	i=1	i=2	i=3	i=4	i=5	i=6
j=1	53-j42(exl)	249(exl)	0(exl)	0(exl)	0(exl)	-9 (exl)
	58-j46(exh)	248(exh)	0(exh)	0(exh)	0(exh)	-9 (exh)
	0(id)	229(id)	0(id)	0(id)	0(id)	-9(id)
j=2	249(exl)	17-j42(exl)	151(exl)	0(exl)	62(exl)	6(exl)
	248(exh)	16-j42(exh)	152(exh)	0(exh)	63(exh)	6(exh)
	229(id)	0(id)	155(id)	0(id)	61(id)	0(id)
j=3	0(exl)	151(exl)	26-j42(exl)	-224(exl)	20(exl)	0(exl)
	0(exh)	152(exh)	26-j42(exh)	-226(exh)	22(exh)	0(exh)
	0(id)	155(id)	0(id)	-206(id)	0(id)	0(id)
j=4	0(exl)	0(exl)	-224(exl)	-22-j44(exl)	151(exl)	0(exl)
	0(exh)	0(exh)	-226(exh)	-26-j40(exh)	150(exh)	0(exh)
	0(id)	0(id)	-206(id)	0(id)	155(id)	0(id)
j=5	0(exl)	62(exl)	20(exl)	151(exl)	14-j43(exl)	249(exl)
	0(exh)	63(exh)	22(exh)	150(exh)	15-j42(exh)	248(exh)
	0(id)	61(id)	0(id)	155(id)	0(id)	229(id)
j=6	-9 (exl)	6(exl)	0(exl)	0(exl)	249(exl)	52-j43(exl)
	-9 (exh)	6(exh)	0(exh)	0(exh)	248(exh)	54-j44(exh)
	-9(id)	0(id)	0(id)	0(id)	229(id)	0(id)
Q_1	32.4602(exl)				32.6213(exl)	
	32.9904(exh)			Q_2	32.9268(exh)	
	36.5880(id)				36.5880(id)	

IV. COMMENTS

The methodology proposed in this work is able to cancel the additional phase shift in the S-parameters. Thus, it has direct application in the extraction of the coupling matrix of two-port resonant filters. When compared to existing methodologies, it may be observed that the new method offers greater flexibility. For example, unlike the methods given in references [3], [7] and [8], the proposed method does not require S-parameters with a wide range. This may be observed in Examples A, B and C, where the frequency range is at least 1.36 times bigger than the filter bandwidth. To achieve a similar result, references [3], [7] and [8] demand frequency ranges 3 to 6 times bigger than the filter bandwidth. In addition, when compared to references [4]-[6], the new method is simpler and presents a better performance, since [4]-[6] includes the inversion of the extracted coupling matrix in order to obtain an error function to be minimized. These latter characteristics may easily cause the method to become unfeasible in the case of high order filters.

The authors also point that although it is shown four decimal places after the comma for the angles in Sec III, Items A, B and C, the method's internal calculations will use the maximum number of decimal places available according to the programming language in which it is implemented. Anyway, it is possible to verify that two decimal places after the comma is good for the angles, whereas the decimal places offered by the most programming languages is good for the others method variables.

V. CONCLUSION

The proposed method may be applied to two-port resonant devices in situations where the available S-parameters have a narrow range of values. The application of this method is, for example, well

justified in the case of filter tuning applications, where the tuning processes are based on extracting a coupling matrix from a simulation. Our method is able to reduce the total time since it operates very well using lower frequency ranges. Thus, the proposed method may be more suitable than [3], [7] and [8] in similar situations. In addition, the proposed method overcomes the convergence issues of [4]-[6], since it does not involve any matrix inversion operations. Lastly, it proved to be successful even in the presence of losses.

REFERENCES

- [1] R. J. Cameron, "Advanced coupling matrix synthesis techniques for microwave filters," *IEEE Transactions On Microwave Theory And Techniques*, vol. 51, no. 1, pp. 1–10, Jan. 2003.
- [2] H. Hu, and K. L. Wu, "A Generalized Coupling Matrix Extraction Technique for Bandpass Filters With Uneven-Qs," *IEEE Transactions on Microwave Theory and Techniques*, vol. 62, no. 2, pp. 244-251, Feb. 2014.
- [3] M. Meng, and K. L. Wu, "An Analytical Approach to Computer-Aided Diagnosis and Tuning of Lossy Microwave Coupled Resonator Filters," *IEEE Transactions On Microwave Theory And Techniques*, vol. 57, no. 12, pp. 3188-3195, Dec. 2009.
- [4] R. Wang, and J. Xu, "Extracting Coupling Matrix And Unload Q From Scattering Parameters Of Lossy Filters," *Progress In Electromagnetics Research*, vol. 115, pp. 303-315, Jan. 2011.
- [5] R. Wang, L. Zhong, L. Peng, X. Qiang, and X. Zhong, "Diagnosis of Coupled Resonator Bandpass Filters Using VF and Optimization Method," *Progress In Electromagnetics Research M*, vol. 51, pp. 195-203, Jan. 2016.
- [6] R. Wang, and J. Xu, "Computer-Aided Diagnosis of Lossy Microwave Coupled Resonators Filters," *International Journal of RF and Microwave Computer-Aided Engineering*, vol. 21, no. 5, pp. 519-525, Jul. 2011.
- [7] F. Seyfert, L. Baratchart, J. P. Mannorat, S. Bila and J. Sombrin, "Extraction of coupling parameters for microwave filters: Determination of a stable rational model from scattering data," *IEEE MTT-S International Microwave Symposium Digest*, pp. 25-28, Jun. 2003.
- [8] P. Zhao, "Phase De-Embedding of Narrowband Coupled-Resonator Networks by Vector Fitting," *IEEE Transactions On Microwave Theory And Techniques*, pp. 1-8, Jul. 2018.
- [9] B. Gustavsen, and A. Semlyen, "Rational approximation of frequency domain responses by Vector Fitting," *IEEE Transactions on Power Delivery*, vol. 14, no. 3, p. 1052–1061, Jul. 1999.
- [10] C.-K. Liao, C.-Y. Chang and J. Lin, "A Vector-Fitting Formulation for Parameter Extraction of Lossy Microwave Filters," *IEEE Microwave and Wireless Components Letters*, vol. 17, no. 4, pp. 277-279, Apr. 2007.
- [11] D. M. Pozar, *Microwave Engineering*, 4th ed., New York, NY, USA: Wiley, 2011.
- [12] *Nelder-Mead User's Manual*, Consortium Scilab - Digiteo, 2010.
- [13] R. J. Cameron, C. M. Kudsia and R. R. Mansour, *Microwave Filters for Communication Systems Fundamentals, Design and Applications*, 2nd ed. Hoboken, NJ, USA: Wiley, 2018.
- [14] J. S. Hong e M. J. Lancaster, *Microstrip filters for RF/Microwave applications*, New York, NY, USA: John Wiley & Sons, Inc, 2001.